

Radiotherapy Followed by Aurora Kinase Inhibition Targets Tumor-Propagating Cells in Human Glioblastoma

Nan Li^{1,2,3}, Dustin J. Maly⁴, Yvan H. Chanthery^{1,2,5}, Daniel W. Sirkis^{1,2,5}, Jean L. Nakamura^{5,6}, Mitchel S. Berger^{2,5}, C. David James^{2,5}, Kevan M. Shokat⁷, William A. Weiss^{1,2,5}, and Anders I. Persson^{1,2,3}

Abstract

Glioblastoma (GBM) is the most common malignant primary brain tumor. Radiotherapy fails to eliminate subpopulations of stem-like tumor-propagating cells (TPC), resulting in tumor regrowth. To identify kinases that promote TPC self-renewal rather than increasing proliferation in human GBM cultures, we screened a library of 54 nonselective tool compounds and determined their kinase inhibitor profiles *in vitro*. Most compounds inhibited aurora kinase (AURK) activity and blocked TPC self-renewal, while inducing GBM cell polynucleation and apoptosis. To prevent regrowth by TPCs, we used a

priming dose of radiation followed by incubation with the pan-AURK inhibitor VX680 to block self-renewal and induce apoptosis in GBM cultures. In mice xenografted with human GBM cells, radiotherapy followed by VX680 treatment resulted in reduced tumor growth and increased survival relative to either monotherapy alone or VX680 treatment before radiation. Our results indicate that AURK inhibition, subsequent to radiation, may enhance the efficacy of radiotherapy by targeting radio-resistant TPCs in human GBMs. *Mol Cancer Ther*; 14(2): 419–28. ©2014 AACR.

Introduction

Conventional therapy of patients with glioblastoma (GBM) includes surgical removal of the tumor followed by radiotherapy and treatment with alkylating agents. Despite this multimodal treatment approach, tumor regrowth is observed in nearly all cases, with patients usually succumbing to the disease within 6 to 12 months (1). Failure to improve upon this outcome is primarily a consequence of inherent intratumoral cellular and molecular heterogeneity, which confers upon GBM the ability to evolve during treatment (2–4). Among the subpopulation of cells in GBM are highly tumorigenic and treatment-resistant tumor-propagating cells (TPC) that are thought to be especially important in repopulating tumors following treatment (5–8). One such subpopulation, expressing the cell-surface antigen prominin 1 (PROM1, CD133), has been shown to be highly tumorigenic following intracranial

transplantation into immunocompromised NOD-SCID mice (9, 10), and CD133⁺ cells have additionally demonstrated radioresistance as well as reduced sensitivity to the DNA alkylator temozolomide (9, 11). In murine GBMs originating from subventricular zone (SVZ) neural stem cells (NSC), a subpopulation of slow-dividing nestin-expressing tumor cells show temozolomide resistance and underlie regrowth (12). Label-retention studies *in vitro* show that CD133⁺ TPCs from human primary GBMs are slow dividing (13), which, in turn, is thought to be a key factor that contributes to CD133⁺ cell therapy resistance. In patients with GBM, a high proliferative index for CD133⁺ tumor cells is associated with a very poor survival (14). In addition, cell cycling of CD133⁺ GBM cells is influenced by the tumor microenvironment (15), which also evolves in association with treatment. Recent studies have identified many alternative TPC markers in human GBM (16). The cell surface sialoglycoprotein podoplanin (PDPN) shows partial coexpression with CD133 in GBM cultures and tissues (15, 17). A better understanding of the intrinsic and extrinsic factors that regulate TPC cell cycling in GBM is important for achieving improved outcomes for patients with GBM.

Sequencing of the human genome has revealed more than 500 protein kinases in mammalian cells, that activity of which influence a variety of cellular processes, including metabolism, transcription, cell-cycle progression, apoptosis, motility, and differentiation (18). Refinement of kinase small-molecule inhibitors has led to the development of compounds with highly selective activities for specific kinase, and such compounds have been used in numerous clinical trials for treating patients with GBM. Other inhibitors, such as imatinib mesylate, sunitinib, and sorafenib, display multitarget profiles, and have shown efficacy in treating chronic myelogenous leukemia, gastrointestinal stromal tumor, and hepatocellular carcinoma, respectively (19–21). Several protein kinase inhibitors have been identified that reduce GBM TPC

¹Department of Neurology, University of California, San Francisco, California. ²Department of Neurological Surgery and Brain Tumor Research Center, University of California, San Francisco, California. ³Sandler Neurosciences Center, University of California, San Francisco, California. ⁴Department of Chemistry, University of Washington, Seattle, Washington. ⁵Helen Diller Family Comprehensive Cancer Center, University of California, San Francisco, California. ⁶Department of Radiation Oncology, University of California, San Francisco, California. ⁷Chemistry and Chemical Biology Graduate Program, Howard Hughes Medical Institute, University of California, San Francisco, California.

Note: Supplementary data for this article are available at Molecular Cancer Therapeutics Online (<http://mct.aacrjournals.org/>).

Corresponding Author: Anders I. Persson, University of California San Francisco, 675 Nelson Rising Lane, NS-270B, San Francisco, CA 94158. Phone: 415-606-3604; Fax: 415-476-0133; E-mail: Anders.Persson@ucsf.edu

doi: 10.1158/1535-7163.MCT-14-0526

©2014 American Association for Cancer Research.

Li et al.

self-renewal and inhibit TPC tumorigenicity (22–24), though the use of these inhibitors, as monotherapies, ultimately fails due to therapy-resistant subpopulation expansion.

To identify kinases that govern self-renewal capacity in GBM tumorsphere cultures, we synthesized a library of 54 structurally related tool compounds and determined their multikinase inhibition profiles by screening against 40 kinases, using the Ambit kinase platform (25). In testing these compounds against three human GBM cultures, and determined that aurora kinase (AURK) is especially important for TPC self-renewal. This observation prompted our use of the pan-AURK inhibitor VX680, in reducing TPC self-renewal after radiation treatment. In cell culture, as well as in xenograft models, we found that radiation followed by VX680 more effectively induced apoptosis and reduced tumor growth, as compared with either monotherapy. Our results support small-molecule inhibitor targeting of GBM TPCs, subsequent to radiotherapy, for improving radiation antitumor effects, and for improving GBM patient outcomes.

Materials and Methods

Cell culture

Tumor tissue was provided by UCSF's Brain Tumor Research Center Tissue Bank and acquired from biopsies of human patients with GBM. The samples were collected during surgery from patients given consent and deidentified according to the protocol approved by the UCSF Committee on Human Research. Two patient-derived GBMs (SF6969 and SF7192) acquired at UCSF (in 2008, DNA fingerprinted 2009) were dissociated using papain, and cell cultures were established using neurobasal (NBE) media (-A; Invitrogen) supplemented with 1% v/v B27 supplement, 0.5% v/v N2 supplement, 20 ng/mL FGF-2 (Peprotech), 20 ng/mL EGF (Sigma-Aldrich), 2 mmol/L L-glutamine, penicillin/streptavidin, and incubated at 37°C in 5% CO₂. From UCSF investigator David James, we received (in 2010) the well-characterized GS2 GBM cells (from a second recurrence; ref. 26) and primary GBM43 cells (27). Tumorspheres were passaged using enzymatic dissociation with Accutase (Innovative Cell Technologies).

Chemical synthesis and validation of kinase inhibition profiles

A library of 54 multitargeted small-molecule kinase tool compounds was synthesized to generate compounds with diverse serine/threonine and tyrosine kinase selectivity profiles. To identify the kinase selectivity profiles of the generated tool compounds, the KINOMEScan binding assay (consisting of 40 kinases) was used (DiscoverX). All compounds were dissolved in DMSO at an initial concentration of 10 mmol/L.

Proliferation assay

To assess the antiproliferative effects of tool compounds or combinations of VX680 treatment and γ -irradiation, we used 96-well polyornithine/laminin-coated plates, plated 0.3×10^4 GBM cells (6969, GS2, 7192, and GBM43) per well in NBE media, and added 0.1, 1, or 10 μ mol/L concentration of each synthesized tool compound, VX680, or DMSO (control). The DNA content was analyzed after 72 hours using the Cyquant NF proliferation assay (Invitrogen). The assay was performed as previously described (28). In brief, cells were lysed and simultaneously incubated at 37°C with a fluorescent probe to label nonfragmented DNA as an indirect measure of the number of cells. The fluorescence intensity

was measured at Ex/Em + 485/530 nm using a Tecan microplate reader. A standard curve was generated by plotting the number of plated cells (1,000–40,000) against corresponding fluorescent values, resulting in the equation $y = x + 150$, $R^2 = 1$. The number of cells in each sample were calculated using this equation. Experiments were done in triplicates.

Self-renewal assay

To assess sphere-forming ability, tumor cells were plated at 1×10^4 cells/mL in ultralow-adherent 24-well plates. The following day, GBM cells (6969, GS2, 7192, and GBM43) were incubated with 10 μ mol/L of each tool compound or DMSO (control) for 72 hours in NBE media, dissociated with Accutase, and then 200 cells were plated as single cells per well in ultralow-adherent 96-well plates. Ten days later, we quantified the number of secondary spheres. Experiments were performed in triplicates from three separate passages.

Apoptosis assay

Using 96-well polyornithine/laminin-coated plates, we plated 0.3×10^4 6969 GBM cells (or GBM43 cells) per well in NBE media and added 0.1, 1, or 10 μ mol/L concentration of each synthesized tool compound or DMSO (control). As a positive control, we used camptothecin. As a negative control, we used the caspase-3/7 inhibitor Ac-DEVD-CHO. The assay was performed according to instructions from the manufacturer (Senzolyte Homogenous AFC Caspase-3/7 assay kit; Anaspec). In brief, the GBM cells were cultured for 48 hours and 50 μ L/well of caspase-3/7 substrate solution was added to each well. The plates were placed on a shaker at room temperature and the fluorescence intensity was measured 30 minutes later at Ex/Em + 380/500 nm using a Tecan microplate reader. The relative intensities were calculated versus DMSO control. Experiments were done in triplicates.

Immunocytochemistry

Cells were cultured on polyornithine/laminin-coated plates at a density of 1×10^4 cells/cm². Cultured cells were fixed in 4% paraformaldehyde for 10 minutes at 4°C, washed in PBS, and incubated in PBS⁺ (PBS containing 5% donkey serum, 3% BSA, 0.3% Triton-X100) for 30 minutes. Primary antibodies against Ser-10 phosphorylated histone H3 (1:1,000; Millipore) and nestin (1:200; Millipore) were incubated in PBS⁺ overnight at 4°C. Cells were washed and incubated with anti-mouse Alexa488 and anti-rabbit Alexa594 antibodies (1:1,000; both from Invitrogen) for 2 hours at room temperature. After 3 \times PBS (DAPI was included in the second wash), coverslips were mounted using Aquamount (Polysciences). Cells were counted using a Nikon Eclipse E800 fluorescence microscope. The percentage of immunoreactive cells was scored by counting the number of immunoreactive cells in 10 unbiased areas (based on DAPI) in triplicates. Images were taken using a Nikon Eclipse E800 fluorescence microscope.

Immunoblotting

Membranes were blotted with antibodies directed against Ser-10 phosphorylated histone H3 (1:500) and GAPDH (1:5000) from Millipore, histone H3 (1:1000), c-ABL (1:1000), FLT3 (1:1000), AURKA (1:1,000), AURKB (1:1,000) from Cell Signaling Technology, AURKC (1:200; Zymed), and β -tubulin (1:3,000; Calbiochem). Bound antibodies were detected with horseradish peroxidase-linked antibodies against mouse or rabbit IgG (Amersham), followed by ECL (Amersham).

Fluorescence-activated cell sorting

For all three human GBMs (6969, GS2, and 7192), we dissociated tumorspheres using Accutase, washed cells twice in AutoMACS rinsing buffer (Miltenyi Biotech.), and then incubated human GBM cells with rat PDPN-PE (phycoerythrin; 1:50; Angiobio) and CD133-APC (1:20, clone 293C; Miltenyi Biotech.) antibodies for 30 minutes at 4°C in rinsing buffer and FCR human blocking reagent (1:10; Miltenyi Biotech.). The cells were washed twice in rinsing buffer and the cells were analyzed with the flow cytometer. For *in vivo* experiments, we gave an i.p. injection of bromodeoxyuridine (BrdUrd; 50 mg/kg; Sigma-Aldrich) 2 hours before isolation and dissociation of enhanced GFP (EGFP)-labeled GBM43 tumors. Cells were rinsed in buffer and incubated with PDPN-PE antibody for 30 minutes at 4°C before cells were fixed and processed for BrdUrd-APC and 7-aminoactinomycin D according to the manufacturer's protocol (APC-BrdU Flow Kit; BD Biosciences) before analysis using a FACS Calibur flow cytometer (BD Biosciences). As controls, primary antibodies were replaced by isotype-matched antibodies from the same manufacturers. Calculations and preparation of images were performed using FlowJo version 7.6.5 software (Treestar Inc.).

For analysis of cell-cycle phases and apoptosis, cells were dissociated with Accutase, fixed in 70% ethanol at +4°C overnight, nuclei were stained with 5 µg/mL propidium iodide containing 125 U/mL RNase for 30 minutes and analyzed with a FACS Calibur flow cytometer (Becton Dickinson). DNA histograms were modeled offline using Modfit-LT software (Verity Software). Apoptosis was detected by measurement of sub-G₁ fraction.

Magnetic-activated cell sorting

For all three human GBMs (6969, GS2, and 7192), we dissociated 1×10^6 tumor cells using Accutase, washed cells twice in AutoMACS rinsing buffer (Miltenyi Biotech.), and then incubated human GBM cells with rat PDPN-PE (1:50; Angiobio) or CD133-PE (1:20; clone 293C, Miltenyi Biotech.) antibodies for 45 minutes at 4°C in rinsing buffer and FCR human blocking reagent (1:10; Miltenyi Biotech.). The cells were washed three times in rinsing buffer and incubated with microbead-tagged anti-PE antibodies (Miltenyi Biotech.) at 4°C in rinsing buffer with FcR human blocking reagent for 30 minutes. After three washes, we suspended cells in 500 mL rinse buffer and separated by magnetic-activated cell sorting (MACS) using large cell separation (LS)-positive selection columns (Miltenyi Biotech.). The negative (CD133⁻ or PDPN⁻) fraction was depleted from remaining positive cells using a second round of MACS. Self-renewal capacity was assayed as mentioned above.

In vivo therapeutic studies

To study the cooperation of radiotherapy and VX680 treatment on GBM growth *in vivo*, we stereotactically injected 300,000 GBM43 cells expressing luciferase (LUC) into the frontal cortex of 4- to 6-week-old athymic nu/nu mice [(Sim:Ncr) nu/nu mice, Simonsen Laboratories]. Injections were done at a depth of 3 mm and the coordinates were 2-mm anterior and 1.5-mm lateral of the right hemisphere relative to Bregma. We measured body weight and bioluminescence every second day during tumor progression. At day 7, we performed cranial γ -irradiation (5 Gy) to two cohorts

($n = 5$ for each cohort) of xenografted mice. One irradiated cohort received a single daily i.p. injection of VX680 (75 mg/kg; Selleck) days 11 to 15. For two other cohorts ($n = 5$), we administered VX680 starting day 7. Half of the VX680-treated xenografted mice received γ -irradiation on day 15. Bioluminescence was measured using a Xenogen IVIS imager and survival was plotted using Kaplan–Meier curves. Symptomatic mice were sacrificed according to ethical guidelines approved by the UCSF Institutional Animal Care and Use Committee.

Statistical analysis

To identify kinases that are important for self-renewal and/or proliferation in human GBM cultures, we used a library of tool compounds displaying a multikinase profile. We incubated three human GBM cultures (6969, GS2, and 7192) with increasing doses of compounds (0.1–10 µmol/L) to study effects on proliferation and 10 µmol/L to study effects on self-renewal capacity. For some statistical analysis, we focused on the 6969 human GBM cells. Using available data from the Ambit kinase platform, we plotted a heatmap of kinase inhibition (Fig. 2A), clustered on the basis of both kinase targets and compounds. The inhibition scale ranges from 0 to 100 (percentage of, as opposed to the control), and the corresponding color scale is white to blue. For *in vivo* studies (bioluminescence and overall survival, OS), we used one-way ANOVA followed by the Newman-Keul *post hoc* test. Sphere-formation assay and proliferation experiments *in vitro*, we used one-way ANOVA followed by the Tukey *post hoc* test.

Results

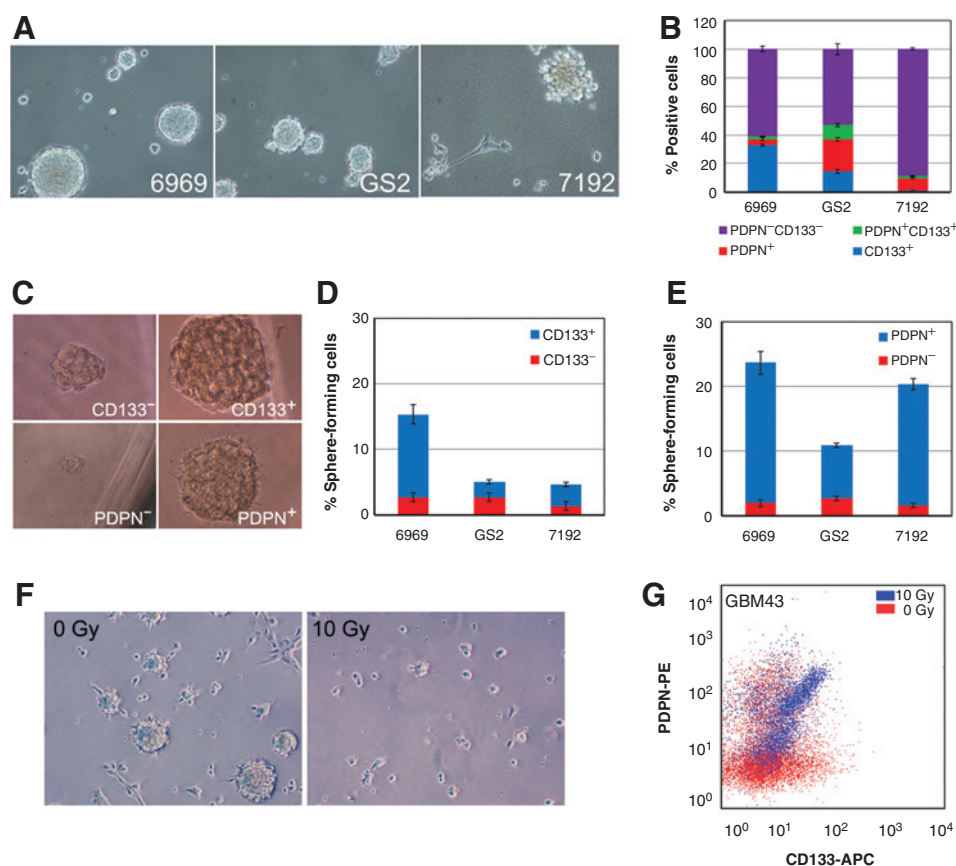
Identifying self-renewing and radioresistant TPCs in human GBM

Previously described human primary GBMs (SF6969 and SF7192) from UCSF, and a secondary GBM GS2 cell line were cultured as tumorspheres in defined media supplemented with growth factors (Fig. 1A; refs. 29, 30). CD133 has previously been suggested as a marker of TPCs in GBM (10). Similar to CD133, previous studies show that hypoxia induces expression of the stem cell marker PDPN, a cell-surface protein associated with increasing grade and worse prognosis in glioma (17, 31). Flow-cytometry experiments demonstrated that subpopulations in all three GBM cultures expressed PDPN and CD133 (Fig. 1B). To test the association of these markers with self-renewal capacity, we collected cells using MACS technology, followed by secondary sphere-formation assays (Fig. 1C). Isolated CD133⁺ cells showed increased self-renewal in 2 of 2 GBM cultures (6969; $P < 0.01$, 7192; $P < 0.055$) compared with CD133⁻ cells (Fig. 1D). In contrast, PDPN⁺ cells show significantly ($P < 0.001$) increased sphere formation compared with PDPN⁻ cells in 3 of 3 GBM cultures (Fig. 1E). To test whether PDPN, similar to CD133 (9), labels radioresistant cells, we exposed cells to a single dose of γ -irradiation (10 Gy; Fig. 1F). Our results show that PDPN is a robust marker of self-renewing and radioresistant TPCs in human GBM (Fig. 1G).

Aurora kinases as therapeutic targets on TPCs in human GBM

The kinase target selectivity profiles of 54 synthesized and structurally related tool compounds were determined using the KINOMEScan screening platform (Fig. 2A). Among other

Li et al.

**Figure 1.**

Podoplanin is a marker of self-renewing and radioresistant human GBM cells. A, three human GBMs (6969, GS2, and 7192) expand as tumorspheres in defined media supplemented with growth factors. B, flow cytometry was used to quantify the overlap of CD133 and PDPN expressions in human GBM cultures. C, to study CD133 and PDPN as markers of self-renewing cells, we plated single cells in 96-well plates for 10 days following dissociation of tumorspheres and MACS isolation. D, a subpopulation of CD133⁺ cells showed slightly increased secondary sphere formation in 2 of 3 GBM cultures compared with CD133⁻ GBM cells. E, PDPN⁺ GBM cells produced significantly more secondary tumorspheres compared with PDPN⁻ cells in 3 of 3 GBM cultures. F, exposure of tumor cells from the well-established GBM43 xenograft to a single dose of γ -irradiation (10 Gy) effectively reduced the numbers of proliferating GBM cells. Most GBM43 cells were synchronously proliferating 4 days following γ -irradiation. G, a single dose of γ -irradiation increased the fraction of PDPN-expressing GBM43 cells (and to lesser extent CD133).

targets, most of the structurally related compounds effectively inhibited AURK activity. To measure activity against bulk tumor cells, we incubated adherent primary human GBM cells (SF6969, SF7192, and GS2) with each kinase inhibitor (0.1–10 μ mol/L, 3d), and quantified proliferation compared with DMSO treated cultures (Fig. 2B). Many compounds inhibited proliferation in a concentration-dependent manner (Fig. 2B). As a measure of apoptosis, we showed that 45 of 54 compounds increased ($P < 0.05$ at 1–10 μ mol/L) cleaved caspase-3/7 activity in 6969 GBM cells compared with DMSO controls (Supplementary Fig. S1A). Although the majority of tumor bulk GBM cells undergo rapid proliferation, an indirect measure of TPCs can be quantified using the secondary tumorsphere formation assay. As a measure of self-renewing TPCs, we incubated tumorspheres with (10 μ mol/L, 3 days), replated dissociated single cells, and scored secondary tumorspheres 10 days later (Fig. 2B). Surprisingly, we found that most compounds blocked self-renewal of TPCs (Fig. 2B). Intriguingly, the structural features of the tool compounds and the inhibitory profiles of kinase activity (Fig. 2A) were reminiscent of the pan-AURK inhibitor VX680 (32). We therefore compared the effects of VX680 and nine structurally related tool compounds (ASC66-73) on proliferation, self-renewal, and apoptosis in human GBM cultures (data not shown). Using well-characterized human GBM43 cells, we confirmed that two tool compounds and VX680 increased ($P < 0.01$) apoptosis compared with DMSO treated cultures (Supplementary Fig. S1B). Quantification showed a concentration-dependent inhibitory effect of VX680 that was less stringent for ASC66 (Fig. 2C

and D). Albeit both ASC66 and VX680 reduced proliferation (VX680, $P < 0.05$ for 0.1–10 μ mol/L; ASC66, $P < 0.05$ for 1–10 μ mol/L), striking inhibitory effects on tumorsphere formation were observed at even lower doses for ASC66 ($P < 0.05$, ASC66 at 0.1 μ mol/L nonsignificant; Fig. 2D). The inhibitory profiles of tool compounds and validation by VX680 suggest that AURKs are necessary for self-renewal of TPCs in human GBMs.

Aurora kinase inhibition reduces the levels of activated histone H3, increases G₂-M arrests, promotes polynucleation, and leads to apoptosis in TPC cultures

To confirm the ability of AURK inhibition to reduce proliferation of TPCs, we demonstrated that VX680 reduced (6969, $P < 0.05$ for 10 nmol/L dose; 6969/GS2, $P < 0.001$ for 100 nmol/L dose) phosphorylated (Ser-10) histone H3 levels in nestin-expressing 6969 and GS2 GBM cells (Fig. 3A–E). We found that all three human GBM cultures expressed AURKA-C, but not some other known targets of VX680 (Supplementary Fig. S2). Incubation of 6969 GBM cells with VX680 or the tool compound ASC58 caused G₂-M arrest, polynucleation, and apoptosis (Fig. 3F–K). As predicted, ASC58 mimicked the cellular effects of VX680 only at higher doses (1 μ mol/L). We confirmed that VX680 concentration dependently reduced phosphorylated histone H3 levels (10 nmol/L, $P < 0.05$; 100 nmol/L, $P < 0.01$) and induced polynucleation (effects mimicked by ASC58 treatment) in human primary GBM43 cells (Supplementary Fig. S3A–S3F). Our results demonstrate that both our synthesized kinase inhibitors expected to target AURKs and VX680 resulted in expected cellular effects,

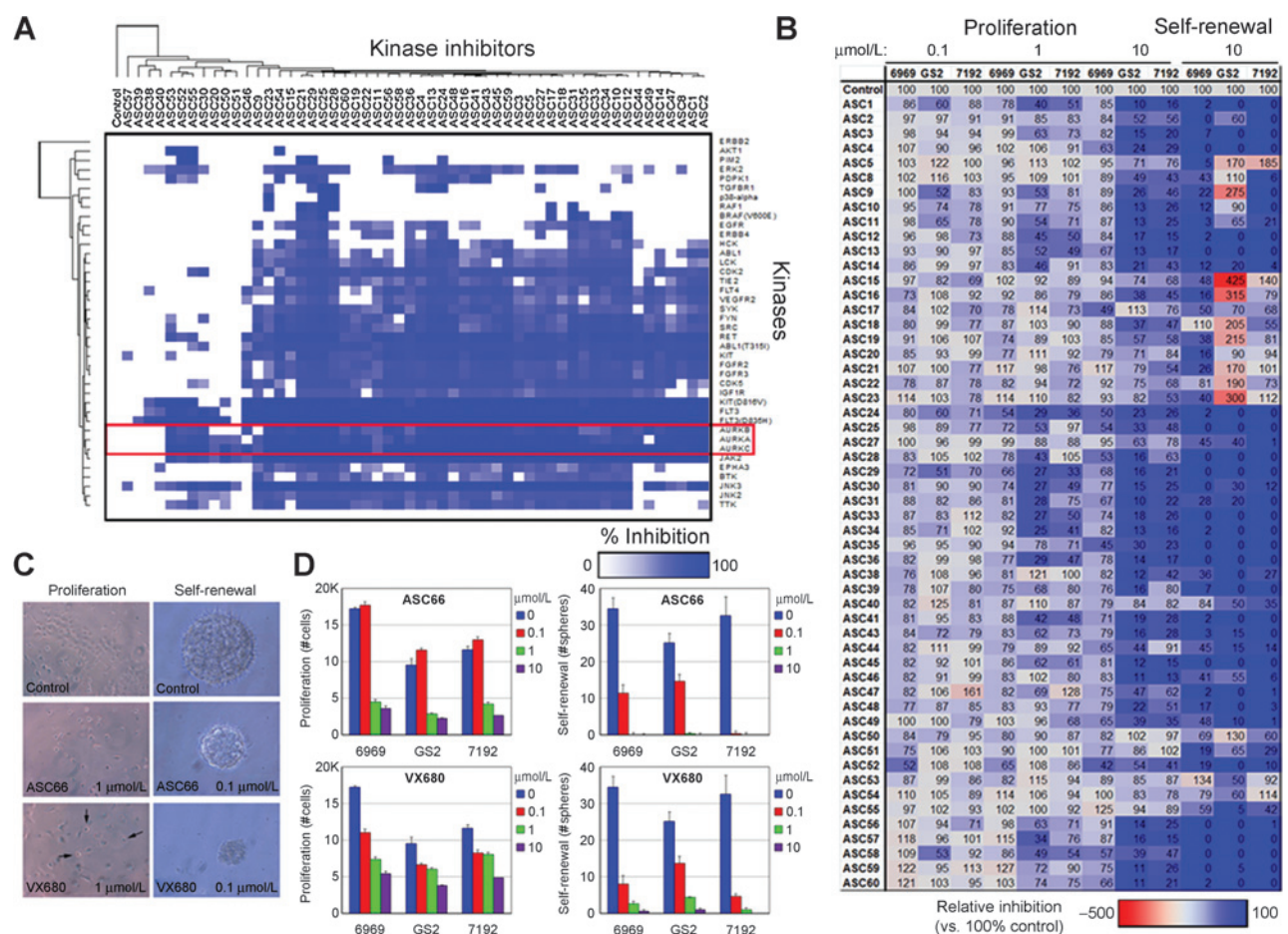


Figure 2.

A multitargeted kinase inhibitor screen identifies AURKs as a therapeutic target in human GBM. A, fifty-four inhibitory multitargeting kinase inhibitors were profiled against 40 kinases using the KINOMEScan screening platform from DiscoverRX. The majority of tool compounds displayed a similar inhibitory kinase profile, including blockade of AURK activity (red box). B, incubation of three human GBM cultures with each tool compound showed a concentration-dependent (0.1-10 $\mu\text{mol/L}$) reduction in proliferation relative to DMSO control (100%). The majority of compounds (10 $\mu\text{mol/L}$) efficiently blocked secondary sphere formation relative to DMSO control (100%). C, the tool compound ASC66 reduced proliferation and self-renewal in human 6969 GBM cultures. The pan-AURK inhibitor VX680 induced arrest in mitosis (arrows) and inhibited self-renewal capacity in human 6969 GBM cultures. D, quantification showed that both ASC66 and VX680 reduced proliferation, but more strikingly blocked self-renewal capacity in human GBM cultures.

including G_2 -M arrest, polynucleation, and apoptosis in human GBMs.

Sequential therapy makes radioresistant TPCs vulnerable to AURK inhibition

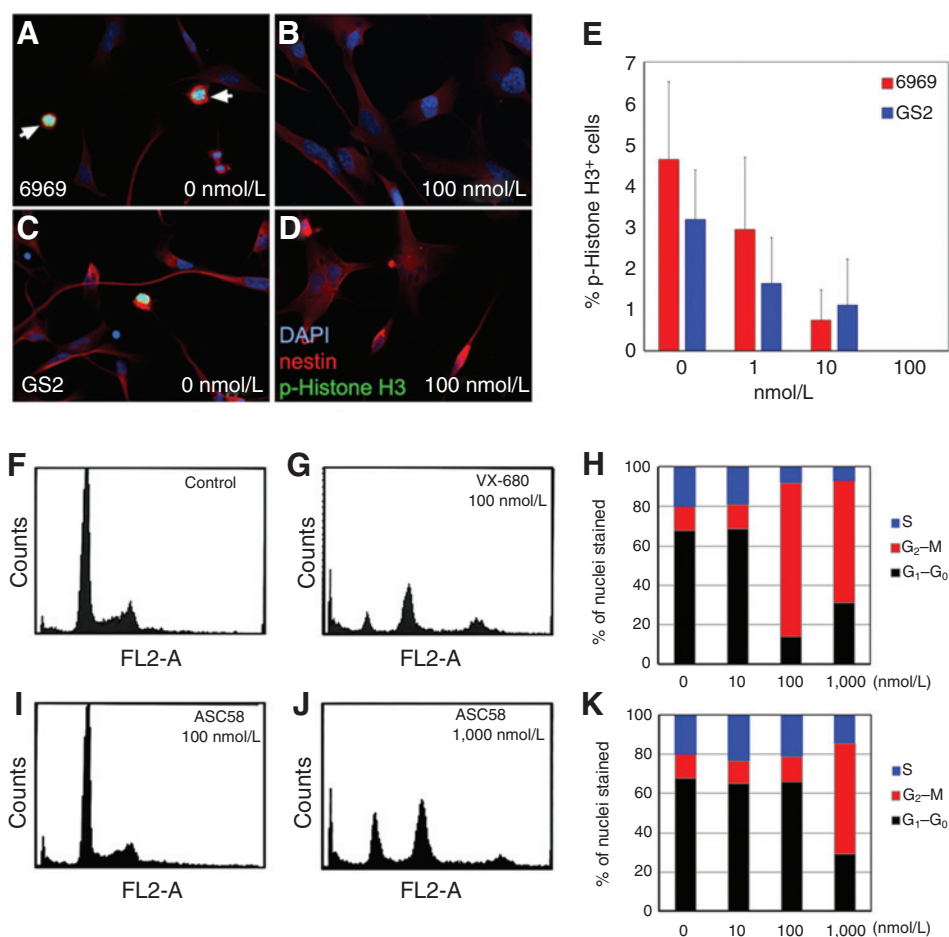
Depletion of tumor bulk cells induced cell cycling of the radioresistant TPC compartment 4 days following a single dose γ -irradiation (Fig. 1G). Therefore, we hypothesize that AURK inhibition for 3 days following a priming dose of radiotherapy will effectively block self-renewal capacity in GBM cultures (Fig. 4A). Proliferation of human primary GBM43 cells was reduced following γ -irradiation (10 Gy, $P < 0.001$) and VX680 treatment (1 $\mu\text{mol/L}$, $P < 0.001$; Fig. 4). However, a priming dose of γ -irradiation followed by AURK inhibition shows no additional inhibition of proliferation compared with γ -irradiation alone (Fig. 4B). In contrast, γ -irradiation increased ($P < 0.001$) and VX680 reduced ($P < 0.01$) the fraction of self-renewing cells forming secondary tumorspheres (Fig. 4B).

VX680 treatment following a priming dose of radiotherapy almost completely abolished generated secondary tumorspheres ($P < 0.001$ vs. control or γ -irradiation, $P < 0.05$ vs. VX680 alone, Fig. 4). Reversal of the sequential treatment regimen (VX680 before γ -irradiation) showed a similar anti-proliferative effect, but less effective at targeting self-renewing TPCs ($P < 0.01$; Supplementary Fig. S4). Our data suggest that induction of cell cycling in TPCs following γ -irradiation optimizes the ability of the AURK inhibitor VX680 to target TPCs in cultured human GBMs.

Sequential therapy reduces tumor growth in mice xenografted with human primary GBM cells

To extend these results to an *in vivo* setting, human primary GBM43 cells expressing firefly luciferase (LUC) gene and EGFP were transplanted orthotopically into athymic *nu/nu* mice (Fig. 5A). One day following a single dose of γ -irradiation (5 Gy), proliferative bulk tumor cells were effectively targeted, and

Li et al.

**Figure 3.**

AURK inhibition produces G₂-M arrest, polynucleation, and apoptosis in human GBM cells. Reduced Ser-10 phosphorylation of histone H3 in (A and B) 6969 and (C and D) GS2 human GBM cultures following incubation with VX680 (100 nmol/L). E, quantification showed that increasing concentrations of VX680 reduce Ser-10 histone H3 phosphorylation in both 6969 and GS2 human GBMs. F-H, the pan-AURK inhibitor VX680 increased the fraction of 6969 GBM cells in G₂-M arrest, induced polynucleation, and resulted in apoptosis. I-K, the tool compound ASC58 (inhibiting AURKB/C among other kinases) mimicked the effects of VX680, albeit at higher doses.

the fraction of PDPN-expressing cells enriched ($P < 0.01$, Fig. 5B and C). To study the ability of VX680 to reduce tumor growth in intracranial xenografts, we confirmed that a single i.p. injection of VX680 (45–75 mg/kg/injection) reduced phosphorylated histone H3 at 48 hours after injection (Fig. 5D). We conclude that VX680 cross the blood–brain barrier (BBB) in our intracranial xenograft model.

To study whether radiotherapy and VX680 can cooperate to reduce tumor growth and prevent regrowth in xenografted mice, we divided mice ($n = 5$) into multiple cohorts (Fig. 5E). Isolation of EGFP⁺ human GBM43 cells from treated mice demonstrated that radiotherapy induced apoptosis (Fig. 5F). Five consecutive and daily injections of VX680 (75 mg/kg/d) induced both G₂-M arrest and polynucleation. Interestingly, administration of VX680 after, but not before, the priming dose of γ -irradiation increased the fraction of apoptotic cells and reduced the fraction of proliferating cells compared with radiotherapy alone (Fig. 5F). Bioluminescence imaging showed that VX680 alone reduced tumor growth without affecting OS; an effect attributed to toxicity and increased body weight loss (Fig. 5G and H and Supplementary Fig. S5). For sequential treatment regimens, we observed that VX680 treatment before, but not after, γ -irradiation resulted in reduced body weight ($P < 0.05$) compared with γ -irradiation alone (Supplementary Fig. S5). Five consecutive injections of VX680 after, but not before, significantly reduced ($P < 0.01$) tumor growth and increased ($P < 0.05$) OS compared with γ -irradiation alone

(Fig. 5G). In conclusion, our *in vivo* results suggest that induction of cell cycling of TPCs through a priming dose of radiotherapy effectively reduce tumor growth and extend OS.

Discussion

Preclinical findings show that a subpopulation of relatively dormant GBM cells is resistant to radiotherapy and temozolomide treatment (9, 11, 12). From a library of multitargeted kinase inhibitors, we confirmed previous findings demonstrating that AURK inhibition effectively reduces proliferation of cultured GBM cells (33, 34). Following a priming dose of ionizing radiation, we demonstrate that AURK inhibitors reduce the self-renewal capacity of TPCs in human GBM cultures. We show that a priming dose of ionizing radiation triggers cell cycling of TPCs *in vivo*, allowing AURK inhibition to induce apoptosis and polynucleation in xenografted GBM43 cells, an effect that was not observed using the AURK inhibitor VX680 alone. Importantly, reversed order of AURK inhibition preceding radiotherapy had no beneficial effect on tumor growth or survival of xenografted mice, suggesting that induced cell cycling of TPCs is a prerequisite for the efficacy of VX680. Administration of the AURKB/C inhibitor AZD1152-HQPA to mice intracranially grafted with the human GBM cell line U251 shows only a moderate survival benefit (33). The authors suggest the possibility that single-agent therapy might fail to target not actively cycling tumor cells and implicate a role

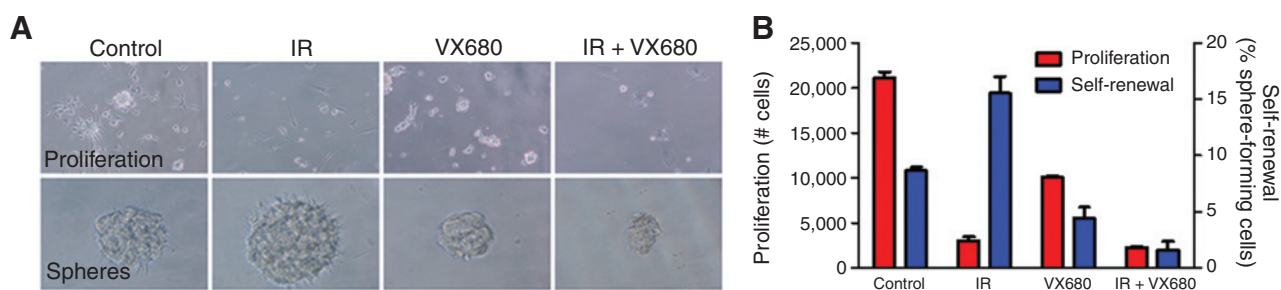


Figure 4.

Radiotherapy-induced cell cycling of TPCs facilitates AURK inhibition and promotes apoptosis in human GBM. To study the effects of radiotherapy and AURK inhibition on proliferation and self-renewal in human GBM43 cells, we tested a sequential therapy regimen [10 Gy radiation followed by VX680 (1 μ mol/L) treatment] compared with vehicle control, radiation, or VX680 (1 μ mol/L) alone. A, radiotherapy and the sequential regimen (γ -irradiation plus VX680 treatment) effectively reduced proliferation compared with VX680-treated or control cultures. The fraction of radioresistant GBM43 cells efficiently showed increased secondary sphere-formation capacity following radiotherapy compared with control cultures. In contrast, VX680, and to a greater extent the sequential regimen, effectively reduced sphere-formation capacity of GBM43 cells compared with control cultures. The few remaining clusters following radiotherapy and VX680 treatment displayed reduced viability. B, quantification showed that γ -irradiation and the sequential regimen effectively reduced proliferation. A less pronounced effect was observed in VX680-only treated cells. The increased fraction of sphere-forming GBM43 cells following γ -irradiation was in stark contrast with the reduced sphere formation in cultures treated with VX680 or a sequential regimen (IR+VX680).

for combination therapy with radiotherapy and temozolomide treatment. Another study found that the AURK inhibitor ZM447439 enhanced the effects of radiotherapy in U251 GBM cells, further potentiated in the presence of temozolomide (35). Our study exemplifies the importance of sequential therapy regimens to target TPC and non-TPC compartments in heterogeneous cancers.

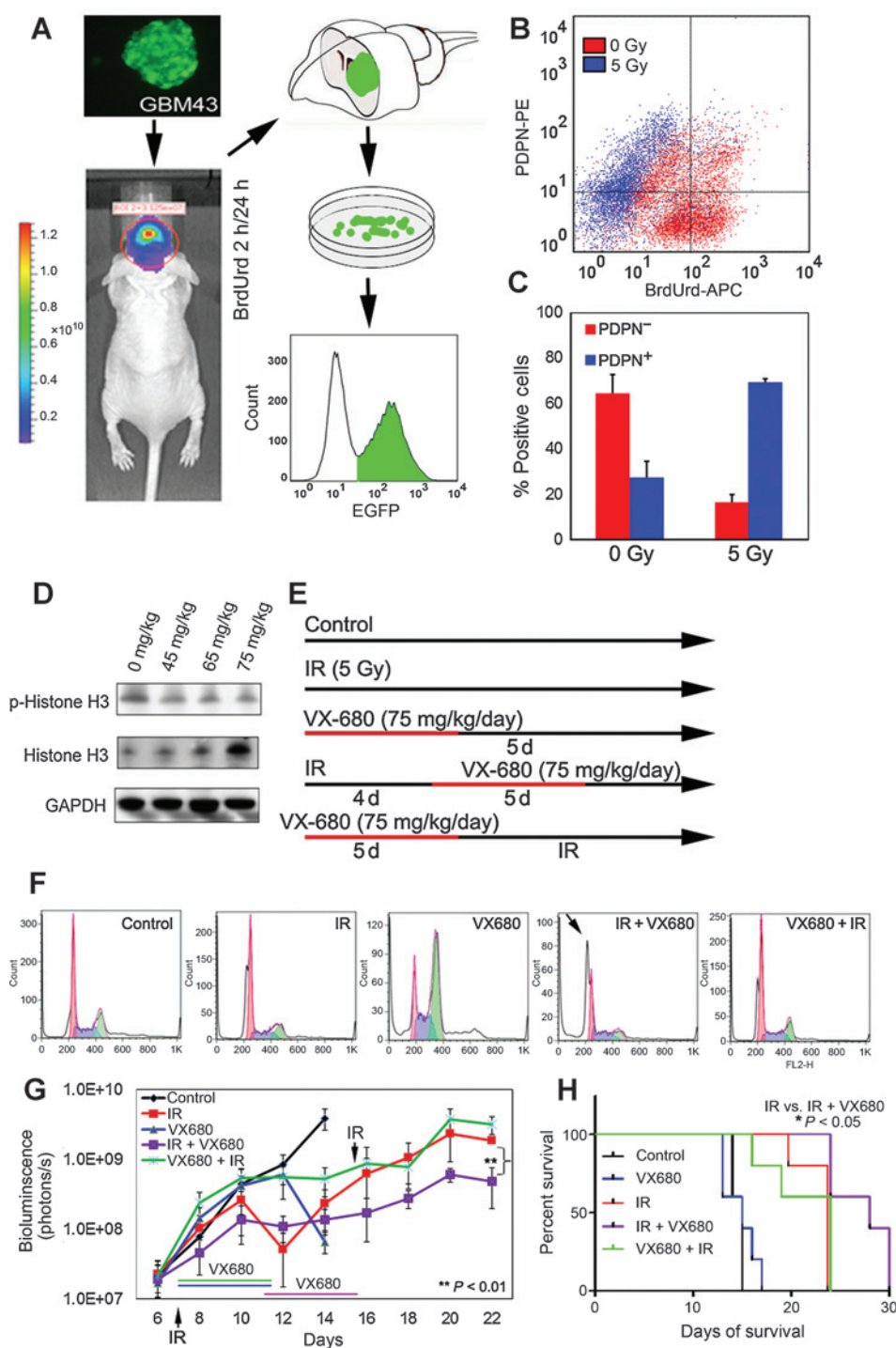
The failure of clinical trials to produce a survival benefit in patients with GBM is due to a multitude of factors, including incomplete surgical removal, off-target effects, poor BBB permeability, and genetic complexity of tumors. The emerging cancer stem cell concept emphasizes the need to better understand how intratumoral heterogeneity contribute to resistance to therapy, and to identify therapeutic targets on TPCs that are thought to underlie regrowth of GBMs and recurrence in patients. The thiazole antibiotic siomycin A was identified through a high-throughput compound screen for inhibitors of the transcription factor forkhead box M1b (FoxM1b; ref. 36). FOXM1 is a critical regulator of a number of genes required for progression through mitosis (37). FOXM1 has been shown to initiate cellular transformation of immortalized human astrocytes and regulate tumorigenicity in human GBM (38). From genome-wide screens aiming to identify genes enriched in multipotent NSCs, the maternal embryonic leucine zipper kinase (MELK) was found and later shown to effectively target TPCs in human GBMs (24). A more recent molecular screen of 31,624 small-molecule inhibitors validated MELK and FOXM1b among seven genes that represent targets on TPC in human GBM (39). The authors recently concluded that phosphorylation of FOXM1 in TPCs is MELK dependent, and that siomycin A improve the response of temozolomide treatment, otherwise failing to target MELK⁺ and FOXM1⁺ GBM cells (40). Interestingly, a screen of GBM xenografts (used in this study) and tumors in patients identified AURKB as one of the overexpressed genes that was tightly associated with also overexpressed FOXM1 (41). On the basis of the multikinase inhibition profile of the tool compounds tested in our study, targeting of CDK2/5, AKT1, FGFR3, AURKB, and AURKC was predicted to most effectively reduce self-renewal of TPCs in cultured human GBMs (Fig. 2B,

data not shown). Beyond the scope of our work, future studies should investigate whether inhibition of individual kinases or combinations effectively reduces self-renewal capacity for TPCs in human GBMs.

All three members of the AURK family play crucial roles at distinct stages of the mitotic phase. Therefore, AURK inhibitors represent an attractive approach to target proliferating GBM cells without affecting nondividing neurons and glial cells (42). The small-molecule pan-AURK inhibitor VX680 is known to suppress tumor growth in animal models (32, 43). In patients with GBM, expression of AURKA in tumors is associated with poor survival (44). *In vitro*, AURKA inhibition in GBM cell lines was cytotoxic and potentiated by ionizing radiation. Interestingly, RNAi of AURKA inhibited self-renewal capacity of TPCs in human primary GBM cultures and reduced tumorigenicity when cells were grafted *in vivo* (45). As a potential therapeutic target in genetically distinct GBM subgroups, AURKB inhibition leads to perturbed cytokinesis, massive polyploidization, and cell death in both TP53-proficient and TP53-deficient cells (46, 47). AURKC is able to reconstitute AURKB function in AURKB-depleted cells (48), suggesting a redundant role during mitosis. AURKB is overexpressed in pediatric diffuse intrinsic pontine gliomas and high-grade gliomas (49). Incubation of pediatric glioma cell lines with VX680 reduced cell survival and resulted in polynucleation. Using GBM cell lines, the AURKB/C-specific inhibitor AZD1152 increased apoptosis and polynucleation *in vitro*, and impaired tumor growth in xenografted GBMs (33, 34). These studies and our results show that correct timing of AURK inhibitors represent a viable approach to target larger cohorts of patients with pediatric or adult glioma.

High interstitial fluid pressure in tumors and selectivity of the BBB against charged molecules contribute to the reduced access of small-molecule inhibitors into human GBMs. Interestingly, a markedly reduced effect of AZD1152-HQPA was demonstrated in intracranially grafted GBMs compared with subcutaneous tumors (33), suggesting limited bioavailability to the brain. We found that a single injection of VX680 was able to reduce Ser-10 phosphorylation of histone H3 and cause

Li et al.

**Figure 5.**

Sequential radiotherapy and AURK inhibition reduce tumor growth in human GBM xenografts. A, human GBM43 cells were lentivirally transduced with GFP and the firefly luciferase (LUC) gene that allowed noninvasive measurements of tumor growth (bioluminescence), efficient isolation, and flow cytometry-mediated identification of tumor cells. B, to study the effect of radiotherapy on dormant and proliferating GBM cells as a function of PDPN expression, we performed radiotherapy, the following day performed i.p. injections of BrdUrd 2 hours before isolation of tumor cells, and then studied overlap of PDPN and BrdUrd using flow cytometry. C, a single dose of γ -irradiation (5 Gy) depleted proliferating tumor cells and markedly increased the fraction of EGFP⁺ PDPN⁺ human GBM43 cells. D, the levels of Ser-10 phosphorylation were reduced 48 hours following a single i.p. injection of VX680 (45–75 mg/kg). E, to test the effects of radiotherapy and VX680 on tumor growth in mice xenografted with GBM43 cells, we divided groups of 5 mice into vehicle control, radiotherapy (IR, 5 Gy), VX680 (75 mg/kg/day \times 5 days), radiotherapy plus VX680, and VX680 followed by radiotherapy. F, we labeled fixed cells with propidium iodide and performed flow-cytometry analysis to study how radiotherapy, VX680, or sequential regimens of radiotherapy and VX680 treatment regulated cell cycling, apoptosis, and polynucleation in tumor cells isolated from treated GBM43 xenografts. G, VX680 resulted in reduced tumor growth in mice xenografted with GBM43 cells compared with untreated (control) mice. Separate cohorts of mice xenografted with GBM43 cells received radiotherapy and two sequential regimens of radiotherapy and VX680 treatment. H, Kaplan-Meier curve showing survival of xenografted mice receiving combinations of γ -irradiation and VX680 treatment.

robust G₂-M arrest in intracranial xenografts of human GBMs (Fig. 5D). As a possible explanation for the improved efficacy of VX680 in xenografted GBMs following ionizing radiation, it is possible that radiotherapy-induced vascular remodeling facilitated uptake of VX680 (Fig. 5G and H). Modification of the chemical structure and alternative delivery of AURK inhibitors are essential for future use against central nervous system tumors.

In conclusion, we anticipate that radiotherapy will remain an integral part of standard of care for patients with GBM. Instead of continuing extensive cycles of radiotherapy (that likely increase radioresistance of resistant TPCs), our study propose that multiple cycles of priming doses of ionizing radiation followed by targeted therapy against proliferating TPCs should inhibit TPC-induced regrowth and recurrence in patients with GBM. The concept of a priming regimen to trigger proliferation

of TPCs has been studied in patients with leukemia (50). Our results show that better understanding of cell-cycling properties in interacting tumor cell compartments should be exploited to eradicate otherwise dormant and resistant TPCs in human GBM.

Disclosure of Potential Conflicts of Interest

No potential conflicts of interest were disclosed.

Authors' Contributions

Conception and design: N. Li, W.A. Weiss, A.I. Persson

Development of methodology: N. Li, D.J. Maly, J.L. Nakamura, C.D. James, K.M. Shokat, A.I. Persson

Acquisition of data (provided animals, acquired and managed patients, provided facilities, etc.): N. Li, Y.H. Chanthery, D.W. Sirkis, A.I. Persson

Analysis and interpretation of data (e.g., statistical analysis, biostatistics, computational analysis): N. Li, Y.H. Chanthery, D.W. Sirkis, W.A. Weiss, A.I. Persson

Writing, review, and/or revision of the manuscript: N. Li, J.L. Nakamura, M.S. Berger, W.A. Weiss, A.I. Persson

Administrative, technical, or material support (i.e., reporting or organizing data, constructing databases): N. Li, M.S. Berger, C.D. James, A.I. Persson

Study supervision: K.M. Shokat, W.A. Weiss, A.I. Persson

References

- Stupp R, Mason WP, van den Bent MJ, Weller M, Fisher B, Taphoorn MJ, et al. Radiotherapy plus concomitant and adjuvant temozolomide for glioblastoma. *N Engl J Med* 2005;352:987–96.
- Johnson BE, Mazar T, Hong C, Barnes M, Aihara K, McLean CY, et al. Mutational analysis reveals the origin and therapy-driven evolution of recurrent glioma. *Science* 2014;343:189–93.
- Snuderl M, Fazlollahi L, Le LP, Nitta M, Zhelyazkova BH, Davidson CJ, et al. Mosaic amplification of multiple receptor tyrosine kinase genes in glioblastoma. *Cancer Cell* 2011;20:810–7.
- Sturm D, Witt H, Hovestadt V, Khuong-Quang DA, Jones DT, Konermann C, et al. Hotspot mutations in H3F3A and IDH1 define distinct epigenetic and biological subgroups of glioblastoma. *Cancer Cell* 2012;22:425–37.
- Al-Hajj M, Wicha MS, Benito-Hernandez A, Morrison SJ, Clarke MF. Prospective identification of tumorigenic breast cancer cells. *Proc Natl Acad Sci U S A* 2003;100:3983–8.
- Bonnet D, Dick JE. Human acute myeloid leukemia is organized as a hierarchy that originates from a primitive hematopoietic cell. *Nat Med* 1997;3:730–7.
- Craddock C, Quek L, Goardon N, Freeman S, Siddique S, Raghavan M, et al. Azacitidine fails to eradicate leukemic stem/progenitor cell populations in patients with acute myeloid leukemia and myelodysplasia. *Leukemia* 2013;27:1028–36.
- Creighton CJ, Li X, Landis M, Dixon JM, Neumeister VM, Sjolund A, et al. Residual breast cancers after conventional therapy display mesenchymal as well as tumor-initiating features. *Proc Natl Acad Sci U S A* 2009;106:13820–5.
- Bao S, Wu Q, McLendon RE, Hao Y, Shi Q, Hjelmeland AB, et al. Glioma stem cells promote radioresistance by preferential activation of the DNA damage response. *Nature* 2006;444:756–60.
- Singh SK, Clarke ID, Terasaki M, Bonn VE, Hawkins C, Squire J, et al. Identification of a cancer stem cell in human brain tumors. *Cancer Res* 2003;63:5821–8.
- Liu G, Yuan X, Zeng Z, Tunici P, Ng H, Abdulkadir IR, et al. Analysis of gene expression and chemoresistance of CD133⁺ cancer stem cells in glioblastoma. *Mol Cancer* 2006;5:67.
- Chen J, Li Y, Yu TS, McKay RM, Burns DK, Kernie SG, et al. A restricted cell population propagates glioblastoma growth after chemotherapy. *Nature* 2012;488:522–6.
- Deleyrolle LP, Harding A, Cato K, Siebzehnubel FA, Rahman M, Azari H, et al. Evidence for label-retaining tumour-initiating cells in human glioblastoma. *Brain* 2011;134:1331–43.
- Pallini R, Ricci-Vitiani L, Banna GL, Signore M, Lombardi D, Todaro M, et al. Cancer stem cell analysis and clinical outcome in patients with glioblastoma multiforme. *Clin Cancer Res* 2008;14:8205–12.
- Christensen K, Schroder HD, Kristensen BW. CD133⁺ niches and single cells in glioblastoma have different phenotypes. *J Neurooncol* 2011;104:129–43.
- Ilkanizadeh S, Lau J, Huang M, Foster DJ, Wong R, Frantz A, et al. Glial progenitors as targets for transformation in glioma. *Adv Cancer Res* 2014;121:1–65.
- Kolenda J, Jensen SS, Aaberg-Jessen C, Christensen K, Andersen C, Brunner N, et al. Effects of hypoxia on expression of a panel of stem cell and chemoresistance markers in glioblastoma-derived spheroids. *J Neurooncol* 2011;103:43–58.
- Manning G, Whyte DB, Martinez R, Hunter T, Sudarsanam S. The protein kinase complement of the human genome. *Science* 2002;298:1912–34.
- Schiffer CA. BCR-ABL tyrosine kinase inhibitors for chronic myelogenous leukemia. *N Engl J Med* 2007;357:258–65.
- Demetri GD, van Oosterom AT, Garrett CR, Blackstein ME, Shah MH, Verweij J, et al. Efficacy and safety of sunitinib in patients with advanced gastrointestinal stromal tumour after failure of imatinib: a randomised controlled trial. *Lancet* 2006;368:1329–38.
- Llovet JM, Ricci S, Mazzaferro V, Hilgard P, Gane E, Blanc JF, et al. Sorafenib in advanced hepatocellular carcinoma. *N Engl J Med* 2008;359:378–90.
- Day BW, Stringer BW, Al-Ejeh F, Ting MJ, Wilson J, Ensley KS, et al. EphA3 maintains tumorigenicity and is a therapeutic target in glioblastoma multiforme. *Cancer Cell* 2013;23:238–48.
- Goidts V, Bageritz J, Puccio L, Nakata S, Zapotka M, Barbus S, et al. RNAi screening in glioma stem-like cells identifies PFKFB4 as a key molecule important for cancer cell survival. *Oncogene* 2012;31:3235–43.
- Nakano I, Masterman-Smith M, Saigusa K, Paucar AA, Horvath S, Shoemaker L, et al. Maternal embryonic leucine zipper kinase is a key regulator of the proliferation of malignant brain tumors, including brain tumor stem cells. *J Neurosci Res* 2008;86:48–60.
- Bamborough P, Drewry D, Harper G, Smith GK, Schneider K. Assessment of chemical coverage of kinome space and its implications for kinase drug discovery. *J Med Chem* 2008;51:7898–914.
- Gunther HS, Schmidt NO, Phillips HS, Kemming D, Kharbanda S, Soriano R, et al. Glioblastoma-derived stem cell-enriched cultures form distinct subgroups according to molecular and phenotypic criteria. *Oncogene* 2008;27:2897–909.
- Giannini C, Sarkaria JN, Saito A, Uhm JH, Galanis E, Carlson BL, et al. Patient tumor EGFR and PDGFRA gene amplifications retained in an

Acknowledgments

The authors thank DiscoverRX KINOMEScan high-throughput kinase selectivity profiling services for screening all the compounds against members of the human kinome. The authors acknowledge the UCSF neurosurgeons and tissue core for providing tumor biopsies from patients with GBM.

Grant Support

This study was supported by NIH/NINDS (U54CA163155 and R21NS088114), the Joel A. Gingras Jr/American Brain Tumor Association (ABTA) Fellowship and Steve Bolser/ABTA Translational Award, the TDC Foundation, and the Guggenheimer Endowment Fund (to A.I. Persson). W.A. Weiss was supported by NIH/NCI/NINDS (U54CA163155 and U01CA176287) and the Waxman Foundation. K.M. Shokat was supported by the Howard Hughes Medical Institute.

The costs of publication of this article were defrayed in part by the payment of page charges. This article must therefore be hereby marked advertisement in accordance with 18 U.S.C. Section 1734 solely to indicate this fact.

Received June 19, 2014; revised November 21, 2014; accepted December 5, 2014; published OnlineFirst December 18, 2014.

Li et al.

- invasive intracranial xenograft model of glioblastoma multiforme. *Neuro Oncol* 2005;7:164–76.
28. Persson AI, Petritsch C, Swartling FJ, Itsara M, Sim FJ, Auvergne R, et al. Non-stem cell origin for oligodendroglioma. *Cancer Cell* 2010;18:669–82.
 29. Chen R, Nishimura MC, Bumbaca SM, Kharbanda S, Forrest WF, Kasman IM, et al. A hierarchy of self-renewing tumor-initiating cell types in glioblastoma. *Cancer Cell* 2010;17:362–75.
 30. Lee J, Kotliarova S, Kotliarov Y, Li A, Su Q, Donin NM, et al. Tumor stem cells derived from glioblastomas cultured in bFGF and EGF more closely mirror the phenotype and genotype of primary tumors than do serum-cultured cell lines. *Cancer Cell* 2006;9:391–403.
 31. Mishima K, Kato Y, Kaneko MK, Nishikawa R, Hirose T, Matsutani M. Increased expression of podoplanin in malignant astrocytic tumors as a novel molecular marker of malignant progression. *Acta Neuropathol* 2006;111:483–8.
 32. Harrington EA, Bebbington D, Moore J, Rasmussen RK, Ajose-Adeogun AO, Nakayama T, et al. VX-680, a potent and selective small-molecule inhibitor of the Aurora kinases, suppresses tumor growth *in vivo*. *Nat Med* 2004;10:262–7.
 33. Diaz RJ, Golbourn B, Shekarforoush M, Smith CA, Rutka JT. Aurora kinase B/C inhibition impairs malignant glioma growth *in vivo*. *J Neurooncol* 2012;108:349–60.
 34. Li J, Anderson MG, Tucker LA, Shen Y, Glaser KB, Shah OJ. Inhibition of Aurora B kinase sensitizes a subset of human glioma cells to TRAIL concomitant with induction of TRAIL-R2. *Cell Death Differ* 2009;16:498–511.
 35. Borges KS, Castro-Gamero AM, Moreno DA, da Silva Silveira V, Brascresco MS, de Paula Queiroz RG, et al. Inhibition of Aurora kinases enhances chemosensitivity to temozolomide and causes radiosensitization in glioblastoma cells. *J Cancer Res Clin Oncol* 2012;138:405–14.
 36. Radhakrishnan SK, Bhat UG, Hughes DE, Wang IC, Costa RH, Gartel AL. Identification of a chemical inhibitor of the oncogenic transcription factor forkhead box M1. *Cancer Res* 2006;66:9731–5.
 37. Kalin TV, Ustiyani V, Kalinichenko VV. Multiple faces of FoxM1 transcription factor: lessons from transgenic mouse models. *Cell Cycle* 2011;10:396–405.
 38. Liu M, Dai B, Kang SH, Ban K, Huang FJ, Lang FF, et al. FoxM1B is overexpressed in human glioblastomas and critically regulates the tumorigenicity of glioma cells. *Cancer Res* 2006;66:3593–602.
 39. Visnyei K, Onodera H, Damoiseaux R, Saigusa K, Petrosyan S, De Vries D, et al. A molecular screening approach to identify and characterize inhibitors of glioblastoma stem cells. *Mol Cancer Ther* 2011;10:1818–28.
 40. Joshi K, Banasavadi-Siddegowda Y, Mo X, Kim SH, Mao P, Kig C, et al. MELK-dependent FOXM1 phosphorylation is essential for proliferation of glioma stem cells. *Stem Cells* 2013;31:1051–63.
 41. Hodgson JG, Yeh RF, Ray A, Wang NJ, Smirnov I, Yu M, et al. Comparative analyses of gene copy number and mRNA expression in glioblastoma multiforme tumors and xenografts. *Neuro Oncol* 2009;11:477–87.
 42. Lens SM, Voest EE, Medema RH. Shared and separate functions of polo-like kinases and aurora kinases in cancer. *Nat Rev Cancer* 2010;10:825–41.
 43. Yang D, Liu H, Goga A, Kim S, Yuneva M, Bishop JM. Therapeutic potential of a synthetic lethal interaction between the MYC proto-oncogene and inhibition of aurora-B kinase. *Proc Natl Acad Sci U S A* 2010;107:13836–41.
 44. Lehman NL, O'Donnell JP, Whiteley LJ, Stapp RT, Lehman TD, Roszka KM, et al. Aurora A is differentially expressed in gliomas, is associated with patient survival in glioblastoma and is a potential chemotherapeutic target in gliomas. *Cell Cycle* 2012;11:489–502.
 45. Xia Z, Wei P, Zhang H, Ding Z, Yang L, Huang Z, et al. AURKA governs self-renewal capacity in glioma-initiating cells via stabilization/activation of beta-catenin/Wnt signaling. *Mol Cancer Res* 2013;11:1101–11.
 46. Ditchfield C, Johnson VL, Tighe A, Ellston R, Haworth C, Johnson T, et al. Aurora B couples chromosome alignment with anaphase by targeting BubR1, Mad2, and Cenp-E to kinetochores. *J Cell Biol* 2003;161:267–80.
 47. Kaestner P, Stolz A, Bastians H. Determinants for the efficiency of anti-cancer drugs targeting either Aurora-A or Aurora-B kinases in human colon carcinoma cells. *Mol Cancer Ther* 2009;8:2046–56.
 48. Sasai K, Katayama H, Stenoien DL, Fujii S, Honda R, Kimura M, et al. Aurora-C kinase is a novel chromosomal passenger protein that can complement Aurora-B kinase function in mitotic cells. *Cell Motil Cytoskeleton* 2004;59:249–63.
 49. Buczkowicz P, Zarghooni M, Bartels U, Morrison A, Misuraca KL, Chan T, et al. Aurora kinase B is a potential therapeutic target in pediatric diffuse intrinsic pontine glioma. *Brain Pathol* 2012;23:244–53.
 50. Lowenberg B, van Putten W, Theobald M, Gmur J, Verdonck L, Sonneveld P, et al. Effect of priming with granulocyte colony-stimulating factor on the outcome of chemotherapy for acute myeloid leukemia. *N Engl J Med* 2003;349:743–52.

Molecular Cancer Therapeutics

Radiotherapy Followed by Aurora Kinase Inhibition Targets Tumor-Propagating Cells in Human Glioblastoma

Nan Li, Dustin J. Maly, Yvan H. Chantry, et al.

Mol Cancer Ther 2015;14:419-428. Published OnlineFirst December 18, 2014.

Updated version Access the most recent version of this article at:
doi:[10.1158/1535-7163.MCT-14-0526](https://doi.org/10.1158/1535-7163.MCT-14-0526)

Supplementary Material Access the most recent supplemental material at:
<http://mct.aacrjournals.org/content/suppl/2014/12/19/1535-7163.MCT-14-0526.DC1>

Cited articles This article cites 50 articles, 13 of which you can access for free at:
<http://mct.aacrjournals.org/content/14/2/419.full#ref-list-1>

Citing articles This article has been cited by 2 HighWire-hosted articles. Access the articles at:
<http://mct.aacrjournals.org/content/14/2/419.full#related-urls>

E-mail alerts [Sign up to receive free email-alerts](#) related to this article or journal.

Reprints and Subscriptions To order reprints of this article or to subscribe to the journal, contact the AACR Publications Department at pubs@aacr.org.

Permissions To request permission to re-use all or part of this article, use this link
<http://mct.aacrjournals.org/content/14/2/419>.
Click on "Request Permissions" which will take you to the Copyright Clearance Center's (CCC) Rightslink site.